



**HAL**  
open science

## Tracing the Fate of Atmospheric Nitrate in a Subalpine Watershed Using $\Delta 17 O$

Ilann Bourgeois, Joel Savarino, Nicolas Caillon, H el ene Angot, Albane Barbero, Franck Delbart, Didier Voisin, Jean-Christophe Clement

### ► To cite this version:

Ilann Bourgeois, Joel Savarino, Nicolas Caillon, H el ene Angot, Albane Barbero, et al.. Tracing the Fate of Atmospheric Nitrate in a Subalpine Watershed Using  $\Delta 17 O$ . *Environmental Science and Technology*, 2018, 52 (10), pp.5561-5570. 10.1021/acs.est.7b02395 . hal-02350366

**HAL Id: hal-02350366**

**<https://hal.science/hal-02350366>**

Submitted on 25 Nov 2020

**HAL** is a multi-disciplinary open access archive for the deposit and dissemination of scientific research documents, whether they are published or not. The documents may come from teaching and research institutions in France or abroad, or from public or private research centers.

L'archive ouverte pluridisciplinaire **HAL**, est destin ee au d ep ot et  a la diffusion de documents scientifiques de niveau recherche, publi es ou non,  emanant des  tablissements d'enseignement et de recherche franais ou  trangers, des laboratoires publics ou priv es.

1           **Tracing the fate of atmospheric nitrate in a subalpine**  
2                           **watershed using  $\Delta^{17}\text{O}$**

3  
4    *Ilann Bourgeois*<sup>1,2,\*</sup>, *Joel Savarino*<sup>1</sup>, *Nicolas Caillon*<sup>1</sup>, *Hélène Angot*<sup>1,a</sup>, *Albane*  
5    *Barbero*<sup>1,b</sup>, *Franck Delbart*<sup>3</sup>, *Didier Voisin*<sup>1</sup>, and *Jean-Christophe Clément*<sup>2,c</sup>

6  
7    <sup>1</sup>Univ. Grenoble Alpes, CNRS, IRD, Grenoble INP, Institut des Géosciences de  
8    l'Environnement, IGE, 38000, Grenoble, France

9    <sup>2</sup>Univ. Grenoble Alpes, CNRS, Laboratoire d'Ecologie Alpine, LECA, 38000,  
10    Grenoble, France

11   <sup>3</sup>Univ. Grenoble Alpes, CNRS, Station Alpine Joseph Fourier, SAJF, 38000,  
12    Grenoble, France

13   <sup>a</sup>Now at Institute for Data, Systems and Society, Massachusetts Institute of  
14    Technology, Cambridge, MA, USA

15   <sup>b</sup>Now at Servicio Meteorológico Nacional - Gerencia Investigación, Desarrollo y  
16    Capacitación, Buenos-Aires, Argentina

17   <sup>c</sup>Now at Univ. Savoie Mont Blanc, INRA, Centre Alpin de Recherche sur les Réseaux  
18    Trophiques des Ecosystèmes Limniques, CARRTEL, 74200, Thonon-Les Bains,  
19    France

20    \*ilann.bourgeois@univ-grenoble-alpes.fr

21  
22    Words count: 5879 (including abstract) / Abstract: 191 words

23    Figures: 4 (1200 words)

24

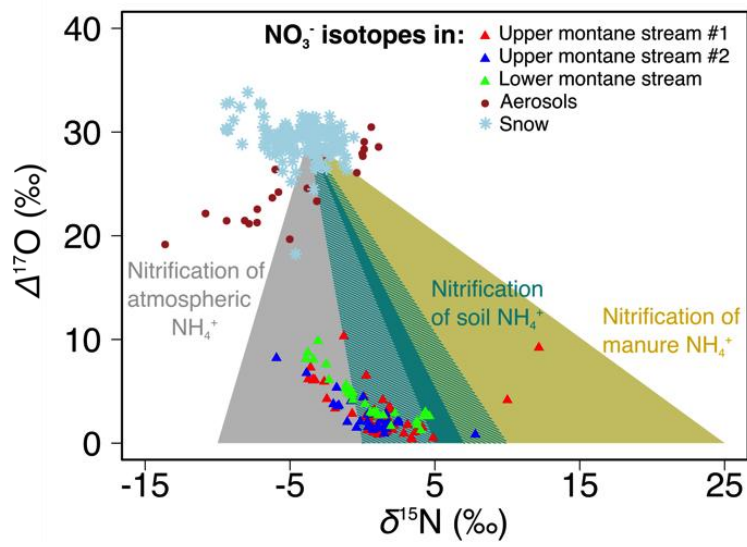
25 **Abstract**

26 Nitrogen is an essential nutrient for life on Earth, but in excess, it can lead to  
27 environmental issues (e.g., N saturation, loss of biodiversity, acidification of lakes,  
28 etc.). Understanding the nitrogen budget (*i.e.*, inputs and outputs) is essential to  
29 evaluate the prospective decay of the ecosystem services (e.g., freshwater quality,  
30 erosion control, loss of high patrimonial-value plant species, etc.) that subalpine  
31 headwater catchments provide, especially as these ecosystems experience high  
32 atmospheric nitrogen deposition. Here, we use a multi-isotopic tracer ( $\Delta^{17}\text{O}$ ,  $\delta^{15}\text{N}$  and  
33  $\delta^{18}\text{O}$ ) of nitrate in aerosols, snow and streams to assess the fate of atmospherically  
34 deposited nitrate in the subalpine watershed of the Lautaret Pass (French Alps). We  
35 show that atmospheric deposition contributes significantly to stream nitrate pool year-  
36 round, either by direct inputs (up to 35 %) or by *in situ* nitrification of atmospheric  
37 ammonium (up to 35 %). Snowmelt in particular leads to high exports of atmospheric  
38 nitrate, most likely fast enough to impede assimilation by surrounding ecosystems.  
39 Yet, in a context of climate change, with shorter snow seasons, and increasing  
40 nitrogen emissions, our results hint at possibly stronger ecological consequences of  
41 nitrogen atmospheric deposition in the close future.

42

43 **Keywords:** atmospheric deposition, nitrate isotopes, subalpine streams, Lautaret  
44 Pass

## TOC



## 45 **1. Introduction**

46 Reactive Nitrogen (Nr) has long been known for its duality. At low to moderate  
47 concentrations, it is an essential nutrient for natural ecosystems in general, and plant  
48 nutrition in particular (1). In excess, Nr becomes an environmental issue for endemic  
49 terrestrial plant species and aquatic ecosystems (2-4), and may pose threats to  
50 human health (5). Human activities have increased N input to the environment by  
51 150% over the last century (6), with a rising contribution – among other distribution  
52 processes – of atmospheric deposition (7,8). Fossil-fuel combustion, agriculture and  
53 food production are responsible for direct or indirect emissions of atmospheric N-  
54 species with the capacity to reach remote ecosystems such as mountainous regions  
55 (9,10) where Nr equilibrium is very sensitive to small perturbations (11,12). Alpine and  
56 subalpine watersheds are particularly vulnerable to this increasing Nr-supply (13,14),  
57 as they are usually N-limited ecosystems (15). The critical load for these ecosystems  
58 has been estimated to 1-4 kg-N.ha<sup>-1</sup>.yr<sup>-1</sup>, making alpine and subalpine grasslands the  
59 most sensitive to N deposition among grasslands and tall forb habitats (16-18). In  
60 some regions of the globe, such as in the Colorado Front Range, USA, shifts from N-  
61 limitation to N-saturation state have been observed leading to regional and national  
62 policies to regulate this phenomenon (19-21). As a consequence of increasing nitrogen  
63 deposition, a slow but persistent change of alpine and subalpine landscape has been  
64 noticed in several regions (22,23). Species more competitive for nitrogen uptake tend  
65 to develop in abundance at the expense of usually oligotrophic native plants, leading  
66 to plant diversity loss and changes in ecosystem functioning and services.

67 Freshwater quality and erosion control are, per instance, threatened by this cascade  
68 of changes (<sup>24,25</sup>). Yet, and mainly because of the paucity of monitoring facilities in  
69 isolated areas and of the logistical difficulties in accessing these regions, key  
70 biogeochemical processes regulating N cycling in mountains are still not well  
71 understood (<sup>26</sup>).

72 More specifically, atmospheric nitrate ( $\text{NO}_3^-$ ) and ammonium ( $\text{NH}_4^+$ ), deriving  
73 principally from anthropogenic  $\text{NO}_x$  ( $\text{NO}$  and  $\text{NO}_2$ ) and agricultural  $\text{NH}_3$  emissions,  
74 are transferred to the land surface through wet and dry deposition. Dissolved  
75 inorganic nitrogen (DIN) species (*i.e.*,  $\text{NO}_3^-$  and  $\text{NH}_4^+$ ) are of capital importance in  
76 ecological studies given their high solubility in water; the strong hydrological  
77 connectivity and typical topography of alpine and subalpine watersheds can lead to a  
78 fast transport and a potentially long reach of the above-mentioned nutrients in  
79 surrounding ecosystems (<sup>27,28</sup>). Traditionally, environmental studies on  $\text{NO}_3^-$  sources  
80 partitioning are essentially based on  $\delta^{15}\text{N}$  and  $\delta^{18}\text{O}\text{-NO}_3^-$  values (<sup>29-31</sup>), to constrain  
81 the biogeochemical processes affecting the various N forms in mountains. Yet, the  
82 wide range of observed values for  $\delta^{15}\text{N}$  and  $\delta^{18}\text{O}\text{-NO}_3^-$  from atmospheric and other  
83 sources limits accurate quantification of contributing sources (<sup>32,33</sup>).

84 In this study we focus – for the first time (to the best of our knowledge) – on year-  
85 round  $\text{NO}_3^-$  dynamics in a mountainous watershed in the French Alps, using a multi-  
86 isotopic ( $\Delta^{17}\text{O}$ ,  $\delta^{18}\text{O}$ ,  $\delta^{15}\text{N}$ ) tracer of  $\text{NO}_3^-$  in subalpine surface waters. This relatively  
87 new method has been increasingly used, as it enables a more refined understanding  
88 of atmospheric  $\text{NO}_3^-$  ( $\text{NO}_3^-_{atm}$ ) contribution to ecosystems N pool (<sup>32,34,35</sup>). With the  
89 aim to clearly delineate the fate of atmospheric N in a subalpine watershed, we first  
90 characterized the triple isotopic composition of  $\text{NO}_3^-$  in aerosols and snow deposited  
91 in high altitude catchments (> 1000m a.s.l.) of the central French Alps (*i.e.*, the input

92 flux). Second, we evaluated the fate of the deposited  $\text{NO}_3^-_{atm}$  by monitoring  $\text{NO}_3^-$   
93 riverine exports from the watersheds (*i.e.*, the output flux).  
94 We hypothesized that (i) the triple isotopes approach will enable a clear delineation  
95 of  $\text{NO}_3^-$  sources and the quantification of their respective contribution to small and  
96 medium-scale watersheds N budget and (ii) seasonal dynamics of  $\text{NO}_3^-_{atm}$  exports in  
97 stream will provide additional insights on N cycling controls in high altitude  
98 catchments.

99

100

## 101 **2. Material and Methods**

### 102 **2.1 Study Site**

103 The studied catchments are located in the upper Romanche valley, near the Lautaret  
104 Pass (central French Alps, SI Figure S1). The experimental site is part of the national  
105 research infrastructure for the study of continental ecosystems and their biodiversity  
106 (AnaEE – France, <https://www.anaee-france.fr>), and of the Long Term Ecological  
107 Research network (LTER, <https://lternet.edu>). The streams monitored throughout  
108 2015 are located close to the research facilities of the Alpine Research Station  
109 (Station Alpine Joseph Fourier (SAJF), CNRS-UGA, UMS 3370,  
110 <https://www.jardinalpindulautaret.fr>), where atmospheric and climatic parameters  
111 were monitored (Figure S2).

112 The climate is subalpine with a strong continental influence. The annual precipitation  
113 in 2015 (year of study) was 537 mm, significantly drier than the mean annual  
114 precipitation of 956 mm observed between 2004 and 2013 (<sup>36</sup>). In 2015, *ca.* 45 % of  
115 the precipitation occurred during the growing season from snowmelt (in April) to late  
116 September. Winters are cold and snowy. The mean temperature was -7.5 °C in

117 February 2015 and 13.9 °C in July 2015. More detailed information about the  
118 sampling site can be found elsewhere (<sup>36,37</sup>).

119 The first studied sub-watershed (hereafter called Lautaret) is mainly constituted of  
120 calcareous substrate and extends over 3.4 km<sup>2</sup>. At the outlet of this sub-watershed  
121 runs a stream called Tufiere. Samples were collected at an altitude of ca. 2015 m  
122 a.s.l, just before the stream merges with the outlet of the second sampled watershed  
123 (Figure S1). Altitude on this watershed spans from 1665 to 2725 m a.s.l. Mean slope  
124 is 25%, and the vegetation cover Normalized Difference Vegetation Index (NDVI) is  
125 0.38.

126 The second sub-watershed (hereafter called Laurichard) is constituted of granitic  
127 rocks on an ancient volcanic layer and extends over 5.3 km<sup>2</sup>. It is part of the North  
128 exposed side of the Combeynot mountain range, which highest peak culminates at  
129 3155 m. The Laurichard stream, fed in part by glacier melt, runs down this  
130 mountainous area and is sampled downhill, just before it joins the Tufiere stream.  
131 Altitude on this watershed ranges from 1665 to 3155 m a.s.l. Mean slope is 30%, and  
132 the vegetation cover NDVI is 0.33.

133 The last river is Romanche, which integrates the response of the whole Romanche  
134 Valley, and is fueled by smaller tributaries such as Tufiere and Laurichard from the  
135 Lautaret Pass and the Ecrins National Park down to the artificial Chambon Lake. Our  
136 sampling point for this river is about 1000 m lower in altitude and approximately 12  
137 km away from the first two tributaries (contributing area  $\approx$  220 km<sup>2</sup>).

138

## 139 **2.2 Field sampling**

140 Aerosols were collected on the Lautaret watershed from November 2014 to  
141 September 2015 using a homemade apparatus (similar to a Digital<sup>®</sup> DA77) equipped



142 with a DigiteI<sup>®</sup> PM2.5 cutting head. We used QMA Whatman quartz filters for  
143 aerosols collection, burnt at 800 °C for 1 h to lower the blank signal (<sup>38</sup>). Filters were  
144 changed on a weekly basis, thus accumulating enough material for isotopic analysis.  
145 Airflow was fixed at 0.5 m<sup>3</sup> per hour.

146 From December 2014 to April 2015 a snow pit (SP) was dug every month on the  
147 Lautaret watershed to provide profiles of NO<sub>3</sub><sup>-</sup><sub>atm</sub> concentration and isotopic values in  
148 the snowpack. For each pit, snow was dug until the soil was reached, then after  
149 cleaning the vertical profile, samples were collected every 3 cm starting from surface  
150 snow.

151 Water samples were collected in the three streams (SI Figure S1, in red) from  
152 November 2014 to December 2015 to obtain a full one-year hydrological cycle and  
153 stream N chemistry. The samples were taken according to the Niwot Ridge LTER  
154 protocol (<sup>39</sup>). Samples were taken on a weekly basis when possible, and at most 2  
155 weeks separated two consecutive samples.

156 More details regarding aerosols, snow and water sampling can be found in the SI,  
157 Appendix 1. Unfortunately, neither rivers discharge measurements nor wet deposition  
158 collection could be done at the time of the study because of the lack of equipment.  
159 Appreciation of snowmelt timeframe, peak and length was based on visual  
160 observation of snow cover and rivers flow. The Laurichard stream could not be  
161 sampled from mid-January to mid-April as the riverbed was completely covered by  
162 the snowpack.

163

### 164 **2.3 Samples pre-treatment and NO<sub>3</sub><sup>-</sup> concentration analysis**

165 Aerosols samples were analyzed by extracting NO<sub>3</sub><sup>-</sup> from filters, immersed in 40 mL  
166 of ultrapure water in a centrifugal ultrafiltration unit (Milipore Centricon plus-70, 100

167 000 Daltons), shaken a few times, and then centrifuged at 4500 RPM for 20 minutes.  
168 The extract was then collected in a 50 mL Corning® centrifuge tube and kept frozen  
169 until further analysis.  
170 Water and snow samples underwent the same pre-treatment for isotopic analysis.  
171 Frozen samples were melted at room temperature overnight before being filtered  
172 using 0.45 µm Whatman GD/X syringe filters linked to a peristaltic pump.  
173 Ultimately, aerosols, snow and stream samples were concentrated using an anionic  
174 resin (0.6 mL AG 1-X8 resin, Cl<sup>-</sup>-form, Bio-Rad) with recovery efficiency over 98.5%  
175 (<sup>40</sup>) and eluted with 10 mL of a 1 M NaCl solution for isotopic analysis (<sup>41</sup>). Sample  
176 aliquots were taken before the resin concentration step for [NO<sub>3</sub><sup>-</sup>] determination using  
177 a Continuous Flow Analysis spectrophotometer (SEAL Analyzer QuAAtro) based on  
178 cadmium-reduction of NO<sub>3</sub><sup>-</sup> to nitrite (<sup>42</sup>). [NO<sub>3</sub><sup>-</sup>] values are given with an uncertainty  
179 of 0.02 mg.L<sup>-1</sup>, calculated as the mean standard deviation of ten successive  
180 measurements of the calibrating standards.

181

## 182 **2.4 Isotopic analysis**

183 Aerosols, snow and river samples were analyzed for  $\Delta^{17}\text{O}$ ,  $\delta^{18}\text{O}$  and  $\delta^{15}\text{N}$  of NO<sub>3</sub><sup>-</sup>  
184 using the bacterial denitrifier technique in combination with the N<sub>2</sub>O gold  
185 decomposition method (<sup>43-45</sup>). More details about the analytical procedure can be  
186 found elsewhere (<sup>46</sup>) and in the SI, Appendix 1.

187 All samples isotopic values were corrected for any isotopic effect possibly occurring  
188 during the procedure by processing simultaneously international reference materials  
189 (International Atomic Energy Agency USGS 32, USGS 34 and USGS 35) through the  
190 same analytical batch. The isotopic standards were prepared in the same  
191 background matrix as samples (*i.e.*, 1M NaCl). Standard deviation of the residuals

192 from the linear regression between the measured reference standards (n = 20) and  
193 their expected values served as indicator of the accuracy of the method. In our study,  
194 the  $\Delta^{17}\text{O}$ ,  $\delta^{18}\text{O}$  and  $\delta^{15}\text{N}$  values of aerosols, snow and streams  $\text{NO}_3^-$  are given, with  
195 respect to atmospheric  $\text{N}_2$  (AIR) and Vienna Standard Mean Ocean Water (VSMOW)  
196 standards, with a mean uncertainty of 0.2, 1.4 and 0.4 ‰ respectively.

197

## 198 **2.5 End-member mixing analysis**

199 The triple stable isotope approach using  $^{18}\text{O}/^{16}\text{O}$  and  $^{17}\text{O}/^{16}\text{O}$  enables exclusive  
200 quantification of unprocessed  $\text{NO}_3^-_{atm}$ . Because chemical pathways leading to the  
201 production of atmospheric  $\text{NO}_3^-$  involve  $\text{NO}_x$  oxidation by ozone, which is the bearer  
202 of  $^{17}\text{O}$ -excess in the first place, it shows a significant positive deviation from the  
203 terrestrial fractionation line (TFL:  $\delta^{17}\text{O} \approx 0.52 * \delta^{18}\text{O}$ ) (47,48).  $\Delta^{17}\text{O}$  is a quantification of  
204 this deviation from the TFL, calculated as  $\Delta^{17}\text{O} = \delta^{17}\text{O} - 0.52 * \delta^{18}\text{O}$  in the present  
205 work.  $\Delta^{17}\text{O}$  value of atmospheric  $\text{NO}_3^-$  generally ranges between 20 and 35 ‰ in  
206 temperate latitudes (46,49) whereas  $\Delta^{17}\text{O}$  value of  $\text{NO}_3^-$  from all other sources  
207 (industrial fertilizers, nitrification) or biologically processed  $\text{NO}_3^-_{atm}$ , is 0 (32,50). In this  
208 study, we used these two distinct  $\Delta^{17}\text{O}$  values as end-members in a simple mixing  
209 model to quantify unprocessed  $\text{NO}_3^-_{atm}$  proportion in streams. Calculation of  
210 atmospheric contribution, noted  $f_{atm}$ , was derived from the following equation:

211

$$212 \text{ (Eq.1) } \quad \Delta^{17}\text{O-NO}_3^-_{sample} = f_{atm} * \Delta^{17}\text{O-NO}_3^-_{atm} + (1 - f_{atm}) * \Delta^{17}\text{O-NO}_3^-_{bio}$$

213 With  $f_{atm}$  (= % $\text{NO}_3^-_{atm}$ ), the mole fraction of the atmospheric contribution (32),  $\Delta^{17}\text{O-}$   
214  $\text{NO}_3^-_{sample}$  the measured value of  $\Delta^{17}\text{O-NO}_3^-$  in a sample and  $\Delta^{17}\text{O-NO}_3^-_{bio}$  the value  
215 of  $^{17}\text{O}$ -excess of biologically-derived  $\text{NO}_3^-$  ( $\text{NO}_3^-_{bio}$ ).

216

217 As  $\Delta^{17}\text{O-NO}_3^-_{bio} = 0 \text{ ‰}$  (<sup>32</sup>), Eq.1 simplifies to

218

219 (Eq. 2) 
$$f_{atm} = (\Delta^{17}\text{O-NO}_3^-_{sample} / \Delta^{17}\text{O-NO}_3^-_{atm}) * 100$$

220

221 Choice for the atmospheric end-member values of  $\Delta^{17}\text{O-NO}_3^-_{atm}$  is further discussed  
222 in section 4.1.

223 Post-deposition processes such as denitrification or assimilation should enrich  $\delta^{18}\text{O}$   
224 and  $\delta^{15}\text{N}$  along a 2:1 to 1:1 line (<sup>51,52</sup>), but co-occurring soil production of  $\text{NO}_3^-$  by  
225 nitrification can lead to lower enrichment proportions (<sup>53</sup>). The  $\Delta^{17}\text{O}$  value of residual  
226  $\text{NO}_3^-$  are unaffected by post-deposition processes leading to  $\text{NO}_3^-$  loss because it is  
227 independent of the absolute  $\delta^{18}\text{O}$  values (<sup>32</sup>). It therefore provides a robust  
228 quantification of unprocessed  $\text{NO}_3^-_{atm}$ , and subsequently, of  $\text{NO}_3^-_{bio}$  as described in  
229 Eq. 2.

230

## 231 **2.6 Statistical Analysis**

232 We used two non-parametric statistical tests in our study. The choice for non-  
233 parametric tests lies in the small population size of the aerosols (n=26), snow (n=30,  
234 22, 29, 36 and 26 for December, January, February, March and April SP,  
235 respectively), and stream water samples (n=42, 29 and 28 for Tufiere, Laurichard  
236 and Romanche, respectively).

237 A Mann-Whitney test was applied on river samples to determine whether mean  
238 concentrations and isotopic values were significantly different between streams. A  
239 Spearman test was applied to evaluate the correlation between stream water  
240 parameters (typically  $\Delta^{17}\text{O}$ ,  $\delta^{18}\text{O}$ ,  $\delta^{15}\text{N}$  and  $[\text{NO}_3^-]$ ). Differences and correlations were  
241 held significant when the *p* value reached a 0.01 credible interval.

242 All statistical analyses were conducted using R software (v3.2.3).

243

244

### 245 **3. Results**

#### 246 **3.1 Nitrate input to ecosystems: $\text{NO}_3^-_{atm}$**

247 Evolution of mean concentration,  $\Delta^{17}\text{O}$ ,  $\delta^{18}\text{O}$  and  $\delta^{15}\text{N}$  of  $\text{NO}_3^-$  in snow pits  
248 throughout the winter and in aerosols throughout year 2015 can be found in Table 1  
249 and Figure S3. First snow falls occurred mid-November 2014 with several freeze-  
250 thaw events before it started to accumulate. On days of snow pits sample collection,  
251 snowpack depths were 66, 64, 139, 142 and 101 cm in December 2014, January,  
252 February, March and April 2015, respectively. Maximum snow accumulation (ca. 1.6  
253 m) occurred early March 2015 (SI, Appendix 1). By the end of April 2015, the  
254 snowpack had completely melted. In December and January, low  $[\text{NO}_3^-]$  were  
255 measured in all snow pits layers (SI, Figure S3a). In February and March, a peak of  
256  $[\text{NO}_3^-]$  up to  $5 \text{ mg}\cdot\text{L}^{-1}$  between 70 and 90 cm of snow accumulation was recorded.  
257 This peak was also measured in April (orange line in Figure S3), but at a lower depth  
258 (40-60 cm) and to a lesser extent ( $2.7 \text{ mg}\cdot\text{L}^{-1}$ ), due to elution of the snowpack  $\text{NO}_3^-$   
259 by snowmelt water.  $\Delta^{17}\text{O}\text{-NO}_3^-$  in snow varied between 20 and 35 ‰ (SI, Figure  
260 S3b), well within the atmospheric range of  $\text{NO}_3^-$  isotopic values reported in the  
261 literature (<sup>46,54</sup>).  $\delta^{18}\text{O}$  and  $\delta^{15}\text{N}$  values were between 60 and 90 ‰ and -10 and 0 ‰,  
262 respectively (SI, Figure S3c and d), consistent with a reservoir exclusively made of  
263  $\text{NO}_3^-_{atm}$  (<sup>51</sup>). Mean ( $\pm$  standard deviation) isotopic values of snow  $\text{NO}_3^-$  were  $29.3 \pm$   
264  $1.6$ ,  $77.0 \pm 5.6$  and  $-3.6 \pm 1.6$  ‰ for  $\Delta^{17}\text{O}$ ,  $\delta^{18}\text{O}$  and  $\delta^{15}\text{N}$ , respectively.  
265 Mean isotopic values of  $\text{NO}_3^-$  in aerosols were also consistent with other  
266 measurements of particulate  $\text{NO}_3^-$  (<sup>55</sup>), featuring significantly lower mean  $\Delta^{17}\text{O}\text{-NO}_3^-$

267 and  $\delta^{15}\text{N-NO}_3^-$  in summer ( $23.1 \pm 2.4$  and  $-6.5 \pm 3.4$  ‰, respectively) than in winter  
268 ( $28.9 \pm 1.7$  and  $-1.0 \pm 1.7$  ‰, respectively), a temporal pattern discussed in the SI,  
269 Appendix 3. Winter aerosols  $\text{NO}_3^-$  isotopic values were in the range of the snowpack  
270  $\text{NO}_3^-$  values.

271

### 272 **3.2 Nitrate output in rivers**

273 All streams  $[\text{NO}_3^-]$  data can be found in the SI, Table S1. Laurichard showed  
274 significantly higher year-round  $[\text{NO}_3^-]$  compared to the other streams, with a mean  
275 value of  $2.6 \pm 1.3$  mg.L<sup>-1</sup>. Mean annual  $[\text{NO}_3^-]$  was  $0.09 \pm 0.06$  mg.L<sup>-1</sup> and  $1.02 \pm 0.48$   
276 mg.L<sup>-1</sup> in Tufiere and Romanche, respectively. Seasonal variations were similar in all  
277 streams, featuring higher  $[\text{NO}_3^-]$  in late spring and lower  $[\text{NO}_3^-]$  in summer (Figure  
278 1a).

279 Tufiere had the widest range in  $\Delta^{17}\text{O-NO}_3^-$  values, varying from 0.5 to 10.3 ‰, with a  
280 mean value of  $3.2 \pm 2.4$  ‰.  $\Delta^{17}\text{O-NO}_3^-$  values in Laurichard ranged from 0.8 to 8.2  
281 ‰, with a mean value of  $2.8 \pm 1.7$  ‰. In Romanche,  $\Delta^{17}\text{O-NO}_3^-$  values remained  
282 above 3 ‰ for a period spanning several months, with a mean value of  $4.3 \pm 2.3$  ‰  
283 (Figure 1b). Mean  $\Delta^{17}\text{O-NO}_3^-$  was significantly higher in Romanche than in Tufiere  
284 and Laurichard, whereas there was no significant difference between Tufiere and  
285 Laurichard mean  $\Delta^{17}\text{O-NO}_3^-$  (p-value = 0.5).

286 All streams showed similar range for  $\delta^{18}\text{O-NO}_3^-$  and  $\delta^{15}\text{N-NO}_3^-$ , between -5 and 25 ‰  
287 for  $\delta^{18}\text{O-NO}_3^-$  and between -6 and 13 ‰ for  $\delta^{15}\text{N-NO}_3^-$ . Our findings were in the same  
288 range of previously measured  $\text{NO}_3^-$  isotopic values in alpine streams (<sup>31,56,57</sup>).

289

## 290 **4. Discussion**

### 291 **4.1 $\text{NO}_3^-_{atm}$ end-member**

292 Our choice to use snow-NO<sub>3</sub><sup>-</sup> as the atmospheric end-member laid on simple but  
293 robust assumptions. First, snow is a good conservator of atmospheric nitrate in high  
294 accumulation sites (> 30 cm of snow accumulation) and preserves its isotopic  
295 composition (<sup>49,59</sup>). Second, the snowpack is representative of winter bulk deposition,  
296 as it aggregates both wet and dry deposition (<sup>60,61</sup>). Third, most of NO<sub>3</sub><sup>-</sup><sub>atm</sub> measured  
297 in streams was assumed to come from snowmelt, as previously observed in other  
298 seasonally snow-covered catchments (<sup>60,62</sup>). Little temporal variation of NO<sub>3</sub><sup>-</sup>  
299 concentration and isotopic values in snow pits profiles, along with no isotopic  
300 evidence of post-deposition processes further supported this assumption (SI,  
301 Appendix 2, Figures S3 and S4).

302 By inputting mean snow Δ<sup>17</sup>O-NO<sub>3</sub><sup>-</sup> in Eq.2, we obtained:

303

304 (Eq.3) 
$$f_{atm} = (\Delta^{17}\text{O-NO}_3^- \text{ sample} / 29.3) * 100$$

305

306 The error range on  $f_{atm}$  was inferred from snow Δ<sup>17</sup>O-NO<sub>3</sub><sup>-</sup> standard deviation, and  
307 calculated as 2 %.

308 It must be underlined that snow as atmospheric end-member might not account  
309 correctly for wet or dry deposition of NO<sub>3</sub><sup>-</sup> in summer. Wet N deposition has *de facto*  
310 been shown to contribute significantly to freshwaters NO<sub>3</sub><sup>-</sup> contents, either through  
311 direct inputs due to flashy hydrology (<sup>34,56</sup>) or through indirect contribution *via*  
312 enhanced nitrification of atmospheric NH<sub>4</sub><sup>+</sup> (<sup>63</sup>). We show that summer deposition of  
313 NO<sub>3</sub><sup>-</sup> (wet or dry) as atmospheric end-member results in higher calculated NO<sub>3</sub><sup>-</sup><sub>atm</sub>  
314 fraction in streams, up to 6% in this study (SI, Appendix 3). For that reason, all  
315 calculated  $f_{atm}$  values in the following sections must be considered as a lower  
316 estimate of NO<sub>3</sub><sup>-</sup><sub>atm</sub> inputs in this system.

317

#### 318 **4.2 Identification of $\text{NO}_3^-_{bio}$ sources**

319 No correlation was found between  $\Delta^{17}\text{O}-\text{NO}_3^-$  and  $[\text{NO}_3^-]$  in Tufiere, Laurichard and  
320 Romanche (Figure 2a, b and c), indicating that  $\text{NO}_3^-_{atm}$  is not the main contributor to  
321 streams nitrate load on a yearly basis. For all streams,  $\Delta^{17}\text{O}-\text{NO}_3^-$  was significantly  
322 correlated to  $\delta^{18}\text{O}-\text{NO}_3^-$  (Figure 2d, e and f) with the best correlation found in  
323 Romanche. Deviations from linear regressions are attributed to occasionally intense  
324 biological processes affecting  $\delta^{18}\text{O}$  signal but leaving  $\Delta^{17}\text{O}$  intact. Otherwise, the  
325 strong linear correlations observed here suggest that mixing of sources more than  
326 biological processes could explain the observed seasonal variations of  $\text{NO}_3^-$  isotopic  
327 values. As a consequence, by extrapolating this linear relationship to  $\Delta^{17}\text{O}-\text{NO}_3^- = 0$   
328 (*i.e.*, 100 % biologically derived  $\text{NO}_3^-$ ), we can determine the mean  $\delta^{18}\text{O}$  value of  
329  $\text{NO}_3^-_{bio}$  produced in the three watersheds: -6.0, -4.6 and -6.6 ‰ in Tufiere, Laurichard  
330 and Romanche, respectively. These results for  $\text{NO}_3^-_{bio}$  were consistent with other  
331 studies estimation of  $\delta^{18}\text{O}-\text{NO}_3^-_{bio}$  in streams, either calculated *via* the same method  
332 (<sup>32,64</sup>) or deduced from measured  $\delta^{18}\text{O}$  values of soil-water and  $\text{O}_2$ , assuming they  
333 respectively contributed to  $\text{NO}_3^-$ -O accordingly to  $\delta^{18}\text{O}-\text{NO}_3^- = 1/3 (\delta^{18}\text{O}-\text{O}_2) + 2/3$   
334  $(\delta^{18}\text{O}-\text{H}_2\text{O})$  (<sup>51,58</sup>). Note that our approach (*i.e.*,  $\Delta^{17}\text{O}$  vs  $\delta^{18}\text{O}$ ) might yield lower  
335 uncertainty compared to the traditional one (*i.e.*,  $\delta^{18}\text{O}$  calculation) which comes with  
336 a number of assumptions and caveats that are thoroughly dissected elsewhere (<sup>58,65</sup>).  
337 Conversely, we found a significant negative correlation between  $\Delta^{17}\text{O}-\text{NO}_3^-$  and  $\delta^{15}\text{N}-$   
338  $\text{NO}_3^-$  (Figure 2g, h and i) in the three streams, with once again the best fit for  
339 Romanche. With the same method as cited above, we can infer the mean  $\delta^{15}\text{N}-\text{NO}_3^-_{bio}$   
340  $\text{NO}_3^-_{bio}$ : 4.4, 5.0 and 6.1 ‰ in Tufiere, Laurichard and Romanche, respectively. These  
341 values characterizing the  $\text{NO}_3^-_{bio}$  end-member are typical of  $\text{NO}_3^-$  produced from soil



342  $\text{NH}_4^+$  nitrification (<sup>51</sup>). On the other hand, extrapolating this correlation to  $\Delta^{17}\text{O}-\text{NO}_3^- =$   
343 29.3 ‰ (*i.e.*, 100%  $\text{NO}_3^-_{atm}$ ) should give  $\delta^{15}\text{N}-\text{NO}_3^-_{atm}$  and  $\delta^{18}\text{O}-\text{NO}_3^-_{atm}$  consistent  
344 with otherwise measured snow  $\text{NO}_3^-$  isotopic values. We found values of 77.7, 79.0  
345 and 74.7 ‰ for  $\delta^{18}\text{O}-\text{NO}_3^-_{atm}$  in Tufiere, Laurichard and Romanche, respectively,  
346 consistent with the mean  $\delta^{18}\text{O}$  value of 77.0 ‰ measured for snow  $\text{NO}_3^-$  (Table 1).  
347 Surprisingly,  $\delta^{15}\text{N}-\text{NO}_3^-_{atm}$  values of *ca.* -30 ‰ were inferred in all streams, far from  
348 measured  $\delta^{15}\text{N}-\text{NO}_3^-$  in snow and aerosols (Table 1) and from existing literature data  
349 showing a range of  $\delta^{15}\text{N}$  values for  $\text{NO}_3^-$  between -15 and 15 ‰ (<sup>51,66–68</sup>). This  
350 suggested that a two end-members mixing model cannot account for the different  
351 sources of N that might have served as substrate for nitrification in subalpine  
352 meadows, and the subsequent large distribution of  $\delta^{15}\text{N}-\text{NO}_3^-_{bio}$ . Such pattern can  
353 only be explained by an additional source of  $\text{NO}_3^-_{bio}$ , with low  $\delta^{15}\text{N}$  values, leading to  
354 the observed weak slopes in Figures 2g, h and i. By lowering the slopes of the  
355 correlations, this additional source was responsible for the low extrapolated  $\delta^{15}\text{N}-$   
356  $\text{NO}_3^-$  values, which in this case (*i.e.*, three sources) do not correspond to any source  
357 end-member.

358 Similar work in alpine watersheds in the Colorado Front Range suggested that  
359 possible sources of  $\text{NO}_3^-$  in streams, apart from snow  $\text{NO}_3^-_{atm}$ , could be nitrification of  
360 snow  $\text{NH}_4^+$  in the snowpack and in soils during snowmelt, or flushing of soil  $\text{NO}_3^-$   
361 produced under the snowpack during winter (<sup>29</sup>). Nitrification in the snowpack is  
362 highly unlikely; indeed, such a process would have overprinted snow  $\Delta^{17}\text{O}-\text{NO}_3^-$   
363 values, which is not the case here (SI, Figure S3 and Appendix 2). However, the dual  
364 isotopes plot presented in Figure 3 hints at a stronger contribution of atmospheric N  
365 deposition – either as snow or rain – than previously assessed in subalpine  
366 watersheds. Deposition of  $\text{NH}_4^+_{atm}$  in particular was likely to enrich soils N pool, and

367 could account for part of  $\text{NO}_3^-_{bio}$  exported in streams. Snow at the Lautaret Pass has  
368 been shown to hold a non-negligible pool of  $\text{NH}_4^+$  – equivalent to  $\text{NO}_3^-$  pool (<sup>37</sup>) –  
369 whereas undetectable  $[\text{NH}_4^+]$  was monitored in all streams (data not shown)  
370 suggesting that  $\text{NH}_4^+$  released from snow is either adsorbed on clay minerals or  
371 biologically processed. If the entire snow- $\text{NH}_4^+$  pool (if considered about roughly the  
372 same size as snow- $\text{NO}_3^-$  pool) was nitrified in soils and exported as  $\text{NO}_3^-$  into  
373 streams during snowmelt, it would account for as much as 54 and 18 % of  $\text{NO}_3^-_{bio}$   
374 production in Tufiere and Laurichard, respectively (Figure 1b). The additional  $\text{NO}_3^-_{bio}$   
375 exported in streams can only be explained by soil leaching at snowmelt. Strong  
376 microbial activity under the snowpack is not uncommon in cold mountainous regions  
377 (<sup>36,62,69,70</sup>) and could justify the observed pattern. At snowmelt, cold adapted microbial  
378 communities massively turn over when confronted to warmer air temperatures (<sup>71</sup>),  
379 releasing nitrified N from lysed cells into the soils where it leaches towards  
380 groundwater and streams (<sup>72</sup>). Sources of nitrified N under the snowpack may be  
381 related to soil organic matter and litter decomposition (<sup>73</sup>) or soil  $\text{NH}_4^+$  pool resulting  
382 from previous year's N deposits (<sup>29,72</sup>). At this point we cannot conclude which source  
383 contributed the most to  $\text{NO}_3^-_{bio}$  yield, but overwinter isotopic monitoring of N pools  
384 under the snowpack might bring clarification.

385

### 386 **4.3 Seasonal variations of $\text{NO}_3^-_{atm}$ exports**

387 All stream water samples in this study had positive  $\Delta^{17}\text{O}-\text{NO}_3^-$  values, showing  
388 unquestionable inputs of  $\text{NO}_3^-_{atm}$  in all streams year-round (Figure 1b). However,  
389 Tufiere and Laurichard, although sampled at the same altitude, showed different  
390  $\text{NO}_3^-$  export patterns, certainly due to different hydrological behaviors and respective  
391 basins characteristics (<sup>58</sup>).

392  $\text{NO}_3^-$  dynamic in Tufiere were most likely governed by snowmelt. Brief but high peaks  
393 of  $^{17}\text{O}$ -excess of  $\text{NO}_3^-$  in March 2015, coincident with higher  $[\text{NO}_3^-]$ , were attributed to  
394 direct runoff of snowmelt water to the stream (<sup>56,64</sup>). Rapid melting of the lower  
395 watershed snowpack washed away labile  $\text{NO}_3^-_{atm}$  deposits and contributed up to 35  
396 % of the total stream  $\text{NO}_3^-$  pool. Leached  $\text{NO}_3^-_{bio}$  from snow-free soils by subsurface  
397 melt or rain water accounted for both higher  $[\text{NO}_3^-]$  and lower  $\Delta^{17}\text{O}-\text{NO}_3^-$  in the  
398 stream later in spring (<sup>74</sup>). Gentle hillslopes and the calcareous substrate of the  
399 Lautaret sub-watershed were also likely to facilitate snowmelt water infiltration and  
400 mixing with groundwater, a common feature in subalpine catchments (<sup>75</sup>). Starting  
401 early May, a slow but persistent increase in  $\Delta^{17}\text{O}-\text{NO}_3^-$  suggested a resurgence of  
402  $\text{NO}_3^-_{atm}$  loaded water entering the stream, increasing  $\text{NO}_3^-_{atm}$  proportion up to 25 %  
403 again at the end of August. Significantly higher precipitation in May and in August,  
404 compared to the previous months (SI, Figure S2a) could have triggered this  
405 resurgence by filling the aquifer with rain water, thus flushing stored water. The wide  
406 temporal range of this  $\Delta^{17}\text{O}$  increase, encompassing six months from May to  
407 October, is in line with a temporally spread transit time of infiltrated melt water along  
408 an altitude gradient. Direct contribution of rain  $\text{NO}_3^-_{atm}$  was unlikely to explain such  
409 pattern, given the low response of Tufiere  $[\text{NO}_3^-]$  and  $\Delta^{17}\text{O}-\text{NO}_3^-$  to the storm in June  
410 (Figure 1a and b). Considering the basin topography and geology (*i.e.*, gentler slopes  
411 and higher vegetation cover), most rain N inputs were certainly retained in soils or  
412 assimilated before either infiltration or direct runoff of rainwater in Tufiere (<sup>63</sup>).

413 Oppositely,  $\text{NO}_3^-_{atm}$  contributed only between 4 and 15 % of total  $\text{NO}_3^-$  in Laurichard  
414 stream from April to May (Figure 1b), coincident with the snowmelt period for this  
415 northern exposed watershed. Laurichard rock glacier is an actively monitored

416 permafrost-related landform, which increased surface velocities over the past twenty  
417 years hint at increased permafrost temperatures, possibly to the point of thawing (<sup>76</sup>).  
418 Considerably higher year-round  $[\text{NO}_3^-]$  in Laurichard compared to snow-fed Tufiere –  
419 by 1-2 orders of magnitude – suggested that Laurichard  $\text{NO}_3^-$  exports were mainly  
420 driven by increasing soil exposure (<sup>77</sup>) more than any other geomorphic or  
421 biogeographic feature (<sup>78</sup>). Sources of such elevated levels of  $\text{NO}_3^-$ , while still  
422 debated (<sup>79,80</sup>), were likely linked to glaciers retreat and permafrost thawing leading to  
423 enhanced stream solutes fluxes (<sup>81,82</sup>), increased nitrification and/or mobilization of  
424 stored N from disturbed soils (<sup>83</sup>). Steeper slopes (SI, Figure S1), and potentially  
425 increased deposition loading because of increased orographic precipitations (<sup>21</sup>) –  
426 relative to the Lautaret watershed – were certainly responsible for the occasional  
427 higher  $\Delta^{17}\text{O}-\text{NO}_3^-$  peaks, concomitant with rain events (Figure 1b). Lower vegetation  
428 cover – and therefore reduced plant  $\text{NO}_3^-_{\text{atm}}$  uptake– and the poor buffering capacity  
429 of Laurichard watershed granitic bedrock are additional factors that could have  
430 fostered punctually enhanced exports of  $\text{NO}_3^-_{\text{atm}}$  from wet deposition (<sup>77,58</sup>). The  
431 storm in June 2015 (Figure S2) led to the strongest input of  $\text{NO}_3^-_{\text{atm}}$  in this stream,  
432 accounting for 29 % of Laurichard  $\text{NO}_3^-$  pool (Figure 1b). Simultaneous  $\Delta^{17}\text{O}-\text{NO}_3^-$   
433 peaks and  $[\text{NO}_3^-]$  minima in July and September were further evidence of this flashy  
434 hydrology and illustrated stream glacial melt water dilution by rain.

435 Conversely, we did not observe an early snowmelt runoff-linked peak in Romanche  
436 stream water  $\Delta^{17}\text{O}-\text{NO}_3^-$  in spring. Instead,  $\text{NO}_3^-_{\text{atm}}$  contribution increased steadily  
437 from April to July (34 % of  $\text{NO}_3^-_{\text{atm}}$  on July 9<sup>th</sup>) then declined until reaching a baseflow  
438 value of about 5 % of  $\text{NO}_3^-_{\text{atm}}$  during the dormant season. Romanche is the main  
439 stream of the valley, fueled by myriad smaller tributaries like Tufiere and Laurichard.  
440 Lower altitude catchments contributed most in spring, but as air temperature and

441 solar radiation increased in summer, melting snowpack from higher watersheds of  
442 the Ecrins National Park may have led to enhanced  $\text{NO}_3^-_{atm}$  export in Romanche  
443 stream leading to the wide  $\Delta^{17}\text{O}-\text{NO}_3^-$  temporal pattern observed in this stream.  
444 Why  $[\text{NO}_3^-]$  decreased from Laurichard to Romanche is uncertain, but dilution by  
445 snow-fed streams like Tufiere between sampling locations is a possibility. Other  
446 possible sinks include denitrification, in-stream algal and phytoplankton assimilation  
447 or uptake by the riparian vegetation (<sup>85</sup>). Denitrification and assimilation should  
448 discriminate  $\delta^{18}\text{O}$  against  $\delta^{15}\text{N}$  of residual  $\text{NO}_3^-$  following a line with a positive slope  
449 (*i.e.*, enrich the residual nitrate with heavier isotopes), which was not observed in our  
450 study (SI, Figure S5). However, frequent recharge of  $\text{NO}_3^-$  by smaller tributaries such  
451 as Laurichard may have overprinted any biological isotopic signature (<sup>53</sup>).  
452 On all basins, the strong controls seemingly exerted either by snowmelt (Tufiere and  
453 Romanche) or by glacier melt water (Laurichard) on stream  $\text{NO}_3^-_{atm}$  exports  
454 precluded the quantification of the direct  $\text{NO}_3^-_{atm}$  summer deposition contribution.  
455 Summer deposition loads of  $\text{NO}_3^-_{atm}$  to streams were either buffered by vegetation  
456 uptake and/or soil immobilization on Lautaret watershed, subdued by high  $\text{NO}_3^-_{bio}$   
457 except on intense rain events on Laurichard watershed, or combined with the wide  
458 temporal response of the Romanche to snowmelt from uplands. Nevertheless,  
459 summer deposition of  $\text{NH}_4^+_{atm}$  contributed significantly to subalpine soils N pool and  
460 was partly responsible for the  $\text{NO}_3^-_{bio}$  exports in streams.  
461 Simultaneous monitoring of  $\Delta^{17}\text{O}-\text{NO}_3^-$ , streams discharge, water isotopes and  
462 chemical tracers of hydrological paths remain needed to further constrain water  
463 sources and their respective contribution to  $\text{NO}_3^-$  exports in subalpine streams.  
464 Longer monitoring of streams exports is also warranted to better evaluate annual  
465 variability in this subalpine watershed, as year 2015 was significantly drier than

466 previous years at the Lautaret Pass. Hydrological responses to rain events, and  
467 resulting  $\text{NO}_3^-$  export dynamics under different precipitation conditions, need to be  
468 assessed.

469

#### 470 **4.4 Nitrogen saturation and ecological implication**

471 Despite presenting different N export dynamics, all streams shared uninterrupted  
472 presence of  $\text{NO}_3^-$  year-round, with a significant contribution from atmospheric  
473 deposition. In a supposedly N-limited ecosystem, such a pattern was unexpected as  
474 demand for dissolved inorganic nitrogen (DIN) from plants and microbial communities  
475 in spring and summer should have exceeded mobile  $\text{NO}_3^-$  reservoir in soils,  
476 precluding leaching to the streams.

477 Nitrogen saturation has first been evaluated in an ecosystem subjected to increasing  
478 N deposition (<sup>2</sup>). Several stages of saturation have been distinguished, ranging from  
479 0 (N-limited ecosystem) to 3 (fully saturated ecosystem characterized by N-leaching  
480 and higher streams [ $\text{NO}_3^-$ ]). [ $\text{NO}_3^-$ ] in Tufiere and Romanche was within the range of  
481 reported alpine and mountain stream [ $\text{NO}_3^-$ ] (<sup>84</sup>), but [ $\text{NO}_3^-$ ] in Laurichard was higher  
482 than in streams pinned as indicators of stage 2 or 3 (<sup>34</sup>). However, similar seasonal  
483 variations of [ $\text{NO}_3^-$ ] in Tufiere, Laurichard and Romanche – high in spring after  
484 snowmelt, decreasing in summer, then increasing again as air temperature starts  
485 falling down (Figure 1) – were symptomatic of plants and microbial biomasses  
486 working as N sinks during the growing season. Evaluation of N saturation according  
487 to the conceptual model of biological demand exceeded by N supply does not take  
488 into account other drivers of N exports (<sup>58</sup>), and may not be adapted to describe the N  
489 saturation state of subalpine watersheds. Another approach to N saturation has been  
490 described as kinetic N saturation, where the rate of N inputs exceeds the rate of N

491 assimilation in an ecosystem and its remediation capacity, and can lead to intensive  
492 exports of N in streams (<sup>86</sup>). Given the highest percentage of unprocessed  $\text{NO}_3^-_{atm}$   
493 during hydrological events, our results provided additional evidence that catchment  
494 hydrology is certainly responsible for the kinetic N saturation in subalpine  
495 watersheds. Anyhow, assessment of N deposition load could help us estimate  
496 whether the critical threshold has been crossed, as evidenced in other alpine  
497 environments (<sup>17,18,87</sup>), and will be the object of future studies.

498 N inputs at the watershed scale, through  $\text{NO}_3^-_{atm}$  direct contribution or  $\text{NH}_4^+_{atm}$   
499 nitrification, are likely to substantially impact surrounding ecosystems, especially  
500 during the growing season following snowmelt. For instance, the lake Chambon, a  
501 freshwater reservoir fueled by the Romanche stream, which supplies downhill  
502 villages and cities – including Grenoble (163 000 inhabitants) – with drinking water,  
503 showed high  $\text{NO}_3^-_{atm}$  contribution from May to November (up to 25 %, Table S2).  
504 While  $[\text{NO}_3^-]$  in the lake averaged  $2.0 \pm 0.8 \text{ mg.L}^{-1}$  during the growing season, far  
505 below the limit of  $50 \text{ mg.L}^{-1}$  (guideline value from The World Health Organization  
506 translated in the EU Water Framework Directive 2000/60/EC), the presence of  $\text{NO}_3^-_{atm}$   
507  $_{atm}$  in this elevated freshwater reservoir is yet another warning signal of potential  
508 threats due to atmospherically deposited pollutants. Evidence of lakes fertilization by  
509 atmospheric deposition in high altitude watersheds has been demonstrated before  
510 (<sup>88</sup>). Fast cycling dynamics of high atmospheric N<sub>r</sub> in lakes (<sup>89</sup>) can lead to well-  
511 documented ecological consequences such as acidification (<sup>17</sup>), shift of algal and  
512 phytoplankton communities (<sup>90,91</sup>) and disturbance of lakes food web (<sup>92</sup>), and  
513 highlight the necessity to protect critical water resources. In winter, limited  
514 hydrological connectivity between soils and streams cannot explain the year-round  
515 export presence of unprocessed  $\text{NO}_3^-_{atm}$  in subalpine streams, highlighting the

516 potential contribution of groundwater contamination to streams exports. Previous  
517 studies also showed that most alpine and subalpine plants acquire N during  
518 snowmelt (<sup>93</sup>). In traditionally N-poor subalpine ecosystems, increasing inputs of  $\text{NO}_3^-$   
519 *atm* together with climate change could accelerate diversity and composition losses of  
520 plant communities.

521 In a 21<sup>st</sup> century with a shorter snow season, a higher fraction of the yearly deposited  
522  $\text{NO}_3^-$  will be brought to subalpine ecosystems at a slower rate, during the growth  
523 season, instead of abruptly at snowmelt. If  $\text{NO}_3^-$  saturation is indeed kinetic – as our  
524 study suggested – then this climate driven change in  $\text{NO}_3^-$  influx timing could result in  
525 higher  $\text{NO}_3^-$  absorption in the environment, and lead to capacity saturation. This  
526 would come with a wide number of changes in the ecosystem, which have been  
527 extensively detailed elsewhere at a global scale (<sup>2,3,8</sup>), and more specifically in high  
528 altitude catchments (<sup>11,18,92</sup>).

529 These findings emphasize the need for more joint monitoring of subalpine soils and  
530 plant communities, with the objective being a better understanding of atmospheric N  
531 deposition consequences on biogeochemical cycling in these semi-isolated  
532 ecosystems. In particular, prospective studies should continue focusing on potential  
533 synergetic effects of land use management coupled with atmospheric deposition on  
534 ecosystems alteration, to better orient policy makers in N emissions mitigation and  
535 adaptation efforts.

536

537

### 538 **Acknowledgments**

539 This study was supported by grants from the Labex OSUG@2020 (“Investissements  
540 d’avenir” - ANR10 LABX56), the ARC - Environnement Région Rhone-Alpes and the



541 Grenoble-Chambéry DIPEE CNRS. This work also benefited from the National  
542 Research Agency support (“Investissements d’avenir” - ANR11 INBS-0001AnaEE-  
543 Services) and from the SAJF research station (UMR 3370, UGA/CNRS)  
544 infrastructures and competences. The study took place on the long-term ecological  
545 research site Zone Atelier Alpes, a member of the ILTER-Europe. We would like to  
546 thank J.-L. Jaffrezo, F. Masson, V. Lucaire, E. Vince, C. Arnoldi and S. Albertin for  
547 help with either laboratory or field work. We acknowledge J. Renaud for help with  
548 SIG.

549

550

### 551 **Supporting Information**

552 Appendix 1 includes complementary information on sampling and analytic protocols.  
553 Appendix 2 and 3 provide explanation on the choice of snow nitrate as atmospheric  
554 end-member. Figures show the study site (S1), the meteorological conditions at the  
555 Lautaret Pass in 2015 (S2), the concentration and isotopic values of  $\text{NO}_3^-$  in snow  
556 during winter 2014-2015 (S3), correlation plots of snow  $\text{NO}_3^-$  isotopic values (S4) and  
557 a correlation plot of rivers  $\delta^{18}\text{O}$  vs  $\delta^{15}\text{N}-\text{NO}_3^-$  (S5). Tables give  $[\text{NO}_3^-]$  for each  
558 sampling date in Tufiere, Laurichard and Romanche (S1) and in the Chambon Lake  
559 (S2). This information is available free of charge via the Internet at  
560 <http://pubs.acs.org>.

561 **References**

- 562 (1) Epstein, E.; Bloom, A. *Mineral Nutrition of Plants Principles and Perspectives, 2nd*  
563 *Edition.*; John Wiley & Sons, 2016.
- 564 (2) Aber, J. D.; Nadelhoffer, K. J.; Steudler, P.; Melillo, J. M. Nitrogen Saturation in  
565 Northern Forest Ecosystems. *BioScience* **1989**, *39* (6), 378–386.
- 566 (3) Vitousek, P. M.; Aber, J. D.; Howarth, R. W.; Likens, G. E.; Matson, P. A.; Schindler,  
567 D. W.; Schlesinger, W. H.; Tilman, D. G. HUMAN ALTERATION OF THE GLOBAL  
568 NITROGEN CYCLE: SOURCES AND CONSEQUENCES. *Ecol. Appl.* **1997**, *7* (3), 737–750.
- 569 (4) Galloway, J. N.; Aber, J. D.; Erisman, J. W.; Seitzinger, S. P.; Howarth, R. W.;  
570 Cowling, E. B.; Cosby, B. J. The Nitrogen Cascade. *BioScience* **2003**, *53* (4), 341.
- 571 (5) Ward, M. H.; deKok, T. M.; Levallois, P.; Brender, J.; Gulis, G.; Nolan, B. T.;  
572 VanDerslice, J. Workgroup Report: Drinking-Water Nitrate and Health—Recent Findings  
573 and Research Needs. *Environ. Health Perspect.* **2005**, *113* (11), 1607–1614.
- 574 (6) Galloway, J. N.; Dentener, F. J.; Capone, D. G.; Boyer, E. W.; Howarth, R. W.;  
575 Seitzinger, S. P.; Asner, G. P.; Cleveland, C. C.; Green, P. A.; Holland, E. A.; et al. Nitrogen  
576 Cycles: Past, Present, and Future. *Biogeochemistry* **2004**, *70* (2), 153–226.
- 577 (7) Matson, P.; Lohse, K. A.; Hall, S. J. The Globalization of Nitrogen Deposition:  
578 Consequences for Terrestrial Ecosystems. *AMBIO J. Hum. Environ.* **2002**, *31* (2), 113.
- 579 (8) Galloway, J. N.; Townsend, A. R.; Erisman, J. W.; Bekunda, M.; Cai, Z.; Freney, J. R.;  
580 Martinelli, L. A.; Seitzinger, S. P.; Sutton, M. A. Transformation of the nitrogen cycle:  
581 recent trends, questions, and potential solutions. *Science* **2008**, *320* (5878), 889–892.
- 582 (9) Baron, J. S.; Nydick, K. R.; Rueth, H. M.; Lafrancois, B. M.; Wolfe, A. P. High  
583 Elevation Ecosystem Responses to Atmospheric Deposition of Nitrogen in the Colorado  
584 Rocky Mountains, USA. In *Global Change and Mountain Regions*; Huber, U. M., Bugmann,  
585 H. K. M., Reasoner, M. A., Eds.; Beniston, M., Series Ed.; Springer Netherlands: Dordrecht,  
586 2005; Vol. 23, pp 429–436.
- 587 (10) Preunkert, S. A seasonally resolved alpine ice core record of nitrate: Comparison  
588 with anthropogenic inventories and estimation of preindustrial emissions of NO in  
589 Europe. *J. Geophys. Res.* **2003**, *108* (D21).
- 590 (11) Baron, J. S.; Rueth, H. M.; Wolfe, A. M.; Nydick, K. R.; Allstott, E. J.; Minear, J. T.;  
591 Moraska, B. Ecosystem Responses to Nitrogen Deposition in the Colorado Front Range.

- 592 *Ecosystems* **2000**, 3 (4), 352–368.
- 593 (12) Kirchner, M.; Fegg, W.; Römmelt, H.; Leuchner, M.; Ries, L.; Zimmermann, R.;  
594 Michalke, B.; Wallasch, M.; Maguhn, J.; Faus-Kessler, T.; et al. Nitrogen deposition along  
595 differently exposed slopes in the Bavarian Alps. *Sci. Total Environ.* **2014**, 470–471, 895–  
596 906.
- 597 (13) Clark, C. M.; Morefield, P. E.; Gilliam, F. S.; Pardo, L. H. Estimated losses of plant  
598 biodiversity in the United States from historical N deposition (1985–2010). *Ecology*  
599 **2013**, 94 (7), 1441–1448.
- 600 (14) Burns, D. A. The effects of atmospheric nitrogen deposition in the Rocky  
601 Mountains of Colorado and southern Wyoming, USA—a critical review. *Environ. Pollut.*  
602 **2004**, 127 (2), 257–269.
- 603 (15) Kaye, J. P.; Hart, S. C. Competition for nitrogen between plants and soil  
604 microorganisms. *Trends Ecol. Evol.* **1997**, 12 (4), 139–143.
- 605 (16) Bobbink, R.; Hettelingh, J.-P.; Review and revision of empirical critical loads and  
606 dose-response relationships. *Review and revision of empirical critical loads and dose-*  
607 *response relationships: proceedings of an expert workshop, Noordwijkerhout, 23-25 June*  
608 *2010*; RIVM: Bilthoven, 2011.
- 609 (17) Baron, J. S.; Driscoll, C. T.; Stoddard, J. L.; Richer, E. E. Empirical Critical Loads of  
610 Atmospheric Nitrogen Deposition for Nutrient Enrichment and Acidification of Sensitive  
611 US Lakes. *BioScience* **2011**, 61 (8), 602–613.
- 612 (18) Nanus, L.; McMurray, J. A.; Clow, D. W.; Saros, J. E.; Blett, T.; Gurdak, J. J. Spatial  
613 variation of atmospheric nitrogen deposition and critical loads for aquatic ecosystems in  
614 the Greater Yellowstone Area. *Environ. Pollut.* **2017**, 223, 644–656.
- 615 (19) Baron, J. S. Hindcasting nitrogen deposition to determine an ecological critical  
616 load. *Ecol. Appl.* **2006**, 16 (2), 433–439.
- 617 (20) Wolfe, A. P.; Van Gorp, A. C.; Baron, J. S. Recent ecological and biogeochemical  
618 changes in alpine lakes of Rocky Mountain National Park (Colorado, USA): a response to  
619 anthropogenic nitrogen deposition. *Geobiology* **2003**, 1 (2), 153–168.
- 620 (21) Williams, M. W.; Tonnessen, K. A. Critical loads for inorganic nitrogen deposition  
621 in the Colorado Front Range, USA. *Ecol. Appl.* **2000**, 10 (6), 1648–1665.
- 622 (22) Bassin, S.; Volk, M.; Fuhrer, J. Species Composition of Subalpine Grassland is  
623 Sensitive to Nitrogen Deposition, but Not to Ozone, After Seven Years of Treatment.  
624 *Ecosystems* **2013**, 16 (6), 1105–1117.
- 625 (23) McDonnell, T. C.; Belyazid, S.; Sullivan, T. J.; Sverdrup, H.; Bowman, W. D.; Porter,  
626 E. M. Modeled subalpine plant community response to climate change and atmospheric  
627 nitrogen deposition in Rocky Mountain National Park, USA. *Environ. Pollut.* **2014**, 187,  
628 55–64.
- 629 (24) Bowman, W. D.; Gartner, J. R.; Holland, K.; Wiedermann, M. Nitrogen Critical  
630 Loads For Alpine Vegetation And Terrestrial Ecosystem Response: Are We There Yet?  
631 *Ecol. Appl.* **2006**, 16 (3), 1183–1193.
- 632 (25) Chapin, F. S.; Walker, B. H.; Hobbs, R. J.; Hooper, D. U.; Lawton, J. H.; Sala, O. E.;  
633 Tilman, D. Biotic control over the functioning of ecosystems. *Science* **1997**, 277 (5325),  
634 500–504.
- 635 (26) Mast, M. A.; Clow, D. W.; Baron, J. S.; Wetherbee, G. A. Links between N Deposition  
636 and Nitrate Export from a High-Elevation Watershed in the Colorado Front Range.  
637 *Environ. Sci. Technol.* **2014**, 48 (24), 14258–14265.
- 638 (27) Campbell, D. H.; Clow, D. W.; Ingersoll, G. P.; Mast, M. A.; Spahr, N. E.; Turk, J. T.  
639 Nitrogen deposition and release in alpine watersheds, Loch Vale, Colorado, USA. *IAHS*  
640 *Publ.-Ser. Proc. Rep.-Intern Assoc Hydrol. Sci.* **1995**, 228, 243–254.

- 641 (28) Clow, D. W.; Sueker, J. K. Relations between basin characteristics and stream  
642 water chemistry in alpine/subalpine basins in Rocky Mountain National Park, Colorado.  
643 *Water Resour. Res.* **2000**, *36* (1), 49–61.
- 644 (29) Kendall, C.; Campbell, D. H.; Burns, D. A.; Shanley, J. B.; Silva, S. R.; Chang, C. C.  
645 Tracing sources of nitrate in snowmelt runoff using the oxygen and nitrogen isotopic  
646 compositions of nitrate. *IAHS Publ.-Ser. Proc. Rep.-Intern Assoc Hydrol. Sci.* **1995**, *228*,  
647 339–348.
- 648 (30) OHTE, N.; NAGATA, T.; TAYASU, I.; KOHZU, A.; YOSHIMIZU, C. Nitrogen and  
649 oxygen isotope measurements of nitrate to survey the sources and transformation of  
650 nitrogen loads in rivers. **2008**.
- 651 (31) Mayer, B.; Boyer, E. W.; Goodale, C.; Jaworski, N. A.; Van Breemen, N.; Howarth, R.  
652 W.; Seitzinger, S.; Billen, G.; Lajtha, K.; Nadelhoffer, K.; et al. Sources of nitrate in rivers  
653 draining sixteen watersheds in the northeastern US: Isotopic constraints.  
654 *Biogeochemistry* **2002**, *57* (1), 171–197.
- 655 (32) Michalski, G.; Meixner, T.; Fenn, M.; Hernandez, L.; Sirulnik, A.; Allen, E.;  
656 Thiemens, M. Tracing Atmospheric Nitrate Deposition in a Complex Semiarid Ecosystem  
657 Using  $\Delta^{17}\text{O}$ . *Environ. Sci. Technol.* **2004**, *38* (7), 2175–2181.
- 658 (33) Liu, T.; Wang, F.; Michalski, G.; Xia, X.; Liu, S. Using  $^{15}\text{N}$ ,  $^{17}\text{O}$ , and  $^{18}\text{O}$  To  
659 Determine Nitrate Sources in the Yellow River, China. *Environ. Sci. Technol.* **2013**, *47*  
660 (23), 13412–13421.
- 661 (34) Rose, L. A.; Elliott, E. M.; Adams, M. B. Triple Nitrate Isotopes Indicate Differing  
662 Nitrate Source Contributions to Streams Across a Nitrogen Saturation Gradient.  
663 *Ecosystems* **2015**, *18* (7), 1209–1223.
- 664 (35) Tsunogai, U.; Miyauchi, T.; Ohyama, T.; Komatsu, D. D.; Nakagawa, F.; Obata, Y.;  
665 Sato, K.; Ohizumi, T. Accurate and precise quantification of atmospheric nitrate in  
666 streams draining land of various uses by using triple oxygen isotopes as tracers.  
667 *Biogeosciences* **2016**, *13* (11), 3441–3459.
- 668 (36) Legay, N.; Grassein, F.; Robson, T. M.; Personeni, E.; Bataillé, M.-P.; Lavorel, S.;  
669 Clément, J.-C. Comparison of inorganic nitrogen uptake dynamics following snowmelt  
670 and at peak biomass in subalpine grasslands. *Biogeosciences* **2013**, *10* (11), 7631–7645.
- 671 (37) Clement, J. C.; Robson, T. M.; Guillemin, R.; Saccone, P.; Lochet, J.; Aubert, S.;  
672 Lavorel, S. The effects of snow-N deposition and snowmelt dynamics on soil-N cycling in  
673 marginal terraced grasslands in the French Alps. *Biogeochemistry* **2012**, *108* (1–3), 297–  
674 315.
- 675 (38) Jaffrezo, J.-L.; Aymoz, G.; Cozic, J. Size distribution of EC and OC in the aerosol of  
676 Alpine valleys during summer and winter. *Atmospheric Chem. Phys.* **2005**, *5* (11), 2915–  
677 2925.
- 678 (39) Williams, M. W.; Melack, J. M. Solute chemistry of snowmelt and runoff in an  
679 Alpine Basin, Sierra Nevada. *Water Resour. Res.* **1991**, *27* (7), 1575–1588.
- 680 (40) Erbland, J. Contraintes isotopiques sur l'interprétation de l'enregistrement en  
681 nitrate dans la carotte de glace de Vostok, Université de Grenoble, 2011.
- 682 (41) Templer, P. H.; Weathers, K. C. Use of mixed ion exchange resin and the denitrifier  
683 method to determine isotopic values of nitrate in atmospheric deposition and canopy  
684 throughfall. *Atmos. Environ.* **2011**, *45* (11), 2017–2020.
- 685 (42) Wood, E. D.; Armstrong, F. A. J.; Richards, F. A. Determination of nitrate in sea  
686 water by cadmium-copper reduction to nitrite. *J. Mar. Biol. Assoc. U. K.* **1967**, *47* (1), 23.
- 687 (43) Casciotti, K. L.; Sigman, D. M.; Hastings, M. G.; Böhlke, J. K.; Hilkert, A.  
688 Measurement of the Oxygen Isotopic Composition of Nitrate in Seawater and Freshwater  
689 Using the Denitrifier Method. *Anal. Chem.* **2002**, *74* (19), 4905–4912.

- 690 (44) Kaiser, J.; Hastings, M. G.; Houlton, B. Z.; Röckmann, T.; Sigman, D. M. Triple  
691 Oxygen Isotope Analysis of Nitrate Using the Denitrifier Method and Thermal  
692 Decomposition of N<sub>2</sub>O. *Anal. Chem.* **2007**, *79* (2), 599–607.
- 693 (45) Morin, S.; Savarino, J.; Frey, M. M.; Yan, N.; Bekki, S.; Bottenheim, J. W.; Martins, J.  
694 M. F. Tracing the Origin and Fate of NO<sub>x</sub> in the Arctic Atmosphere Using Stable Isotopes  
695 in Nitrate. *Science* **2008**, *322* (5902), 730–732.
- 696 (46) Morin, S.; Savarino, J.; Frey, M. M.; Domine, F.; Jacobi, H.-W.; Kaleschke, L.;  
697 Martins, J. M. F. Comprehensive isotopic composition of atmospheric nitrate in the  
698 Atlantic Ocean boundary layer from 65°S to 79°N. *J. Geophys. Res.* **2009**, *114* (D5).
- 699 (47) Thiemens, M. H. History and applications of mass-independent isotope effects.  
700 *Annu Rev Earth Planet Sci* **2006**, *34*, 217–262.
- 701 (48) Kaiser, J. Technical note: Consistent calculation of aquatic gross production from  
702 oxygen triple isotope measurements. *Biogeosciences* **2011**, *8* (7), 1793–1811.
- 703 (49) Savarino, J.; Kaiser, J.; Morin, S.; Sigman, D. M.; Thiemens, M. H. Nitrogen and  
704 oxygen isotopic constraints on the origin of atmospheric nitrate in coastal Antarctica.  
705 *Atmospheric Chem. Phys.* **2007**, *7* (8), 1925–1945.
- 706 (50) Michalski, G.; Kolanowski, M.; Riha, K. M. Oxygen and nitrogen isotopic  
707 composition of nitrate in commercial fertilizers, nitric acid, and reagent salts. *Isotopes*  
708 *Environ. Health Stud.* **2015**, *51* (3), 382–391.
- 709 (51) Kendall, C.; Elliott, E. M.; Wankel, S. D. Tracing anthropogenic inputs of nitrogen  
710 to ecosystems. *Stable Isot. Ecol. Environ. Sci.* **2007**, *2*, 375–449.
- 711 (52) Granger, J.; Sigman, D. M.; Rohde, M. M.; Maldonado, M. T.; Tortell, P. D. N and O  
712 isotope effects during nitrate assimilation by unicellular prokaryotic and eukaryotic  
713 plankton cultures. *Geochim. Cosmochim. Acta* **2010**, *74* (3), 1030–1040.
- 714 (53) Granger, J.; Wankel, S. D. Isotopic overprinting of nitrification on denitrification as  
715 a ubiquitous and unifying feature of environmental nitrogen cycling. *Proc. Natl. Acad. Sci.*  
716 **2016**, *113* (42), E6391–E6400.
- 717 (54) Savarino, J.; Morin, S.; Erbland, J.; Grannec, F.; Patey, M. D.; Vicars, W.; Alexander,  
718 B.; Achterberg, E. P. Isotopic composition of atmospheric nitrate in a tropical marine  
719 boundary layer. *Proc. Natl. Acad. Sci.* **2013**, *110* (44), 17668–17673.
- 720 (55) Elliott, E. M.; Kendall, C.; Boyer, E. W.; Burns, D. A.; Lear, G. G.; Golden, H. E.;  
721 Harlin, K.; Bytnerowicz, A.; Butler, T. J.; Glatz, R. Dual nitrate isotopes in dry deposition:  
722 Utility for partitioning NO<sub>x</sub> source contributions to landscape nitrogen deposition. *J.*  
723 *Geophys. Res.* **2009**, *114* (G4).
- 724 (56) Campbell, D. H.; Kendall, C.; Chang, C. C. Y.; Silva, S. R.; Tonnessen, K. A. Pathways  
725 for nitrate release from an alpine watershed: Determination using δ<sup>15</sup>N and δ<sup>18</sup>O:  
726 ALPINE WATERSHED NITRATE δ<sup>15</sup>N AND δ<sup>18</sup>O. *Water Resour. Res.* **2002**, *38* (5), 10-1-  
727 10-19.
- 728 (57) Burns, D. A.; Kendall, C. Analysis of δ<sup>15</sup>N and δ<sup>18</sup>O to differentiate NO<sub>3</sub><sup>-</sup> sources  
729 in runoff at two watersheds in the Catskill Mountains of New York. *Water Resour. Res.*  
730 **2002**, *38* (5), 9–1.
- 731 (58) Rose, L. A.; Sebestyen, S. D.; Elliott, E. M.; Koba, K. Drivers of atmospheric nitrate  
732 processing and export in forested catchments. *Water Resour. Res.* **2015**, *51* (2), 1333–  
733 1352.
- 734 (59) Hastings, M. G. Seasonal variations in N and O isotopes of nitrate in snow at  
735 Summit, Greenland: Implications for the study of nitrate in snow and ice cores. *J.*  
736 *Geophys. Res.* **2004**, *109* (D20).
- 737 (60) Williams, M. W.; Seibold, C.; Chowanski, K. Storage and release of solutes from a  
738 subalpine seasonal snowpack: soil and stream water response, Niwot Ridge, Colorado.

- 739 *Biogeochemistry* **2009**, 95 (1), 77–94.
- 740 (61) Campbell, J. L.; Mitchell, M. J.; Mayer, B.; Groffman, P. M.; Christenson, L. M.  
741 Mobility of Nitrogen-15-Labeled Nitrate and Sulfur-34-Labeled Sulfate during Snowmelt.  
742 *Soil Sci. Soc. Am. J.* **2007**, 71 (6), 1934.
- 743 (62) Brooks, P. D.; Williams, M. W. Snowpack controls on nitrogen cycling and export  
744 in seasonally snow-covered catchments. *Hydrol. Process.* **1999**, 13 (14), 2177–2190.
- 745 (63) Nanus, L.; Williams, M. W.; Campbell, D. H.; Elliott, E. M.; Kendall, C. Evaluating  
746 Regional Patterns in Nitrate Sources to Watersheds in National Parks of the Rocky  
747 Mountains using Nitrate Isotopes. *Environ. Sci. Technol.* **2008**, 42 (17), 6487–6493.
- 748 (64) Darrouzet-Nardi, A.; Erbland, J.; Bowman, W. D.; Savarino, J.; Williams, M. W.  
749 Landscape-level nitrogen import and export in an ecosystem with complex terrain,  
750 Colorado Front Range. *Biogeochemistry* **2012**, 109 (1–3), 271–285.
- 751 (65) Snider, D. M.; Spoelstra, J.; Schiff, S. L.; Venkiteswaran, J. J. Stable Oxygen Isotope  
752 Ratios of Nitrate Produced from Nitrification: 18O-Labeled Water Incubations of  
753 Agricultural and Temperate Forest Soils. *Environ. Sci. Technol.* **2010**, 44 (14), 5358–  
754 5364.
- 755 (66) Xue, D.; Botte, J.; De Baets, B.; Accoe, F.; Nestler, A.; Taylor, P.; Van Cleemput, O.;  
756 Berglund, M.; Boeckx, P. Present limitations and future prospects of stable isotope  
757 methods for nitrate source identification in surface- and groundwater. *Water Res.* **2009**,  
758 43 (5), 1159–1170.
- 759 (67) Mara, P.; Mihalopoulos, N.; Gogou, A.; Daehnke, K.; Schlarbaum, T.; Emeis, K.-C.;  
760 Krom, M. Isotopic composition of nitrate in wet and dry atmospheric deposition on Crete  
761 in the eastern Mediterranean Sea: ISOTOPIC COMPOSITION OF NITRATE IN  
762 DEPOSITION. *Glob. Biogeochem. Cycles* **2009**, 23 (4), n/a-n/a.
- 763 (68) Guha, T.; Lin, C. T.; Bhattacharya, S. K.; Mahajan, A. S.; Ou-Yang, C.-F.; Lan, Y.-P.;  
764 Hsu, S. C.; Liang, M.-C. Isotopic ratios of nitrate in aerosol samples from Mt. Lulin, a high-  
765 altitude station in Central Taiwan. *Atmos. Environ.* **2017**, 154, 53–69.
- 766 (69) Jusselme, M.-D.; Saccone, P.; Zinger, L.; Faure, M.; Le Roux, X.; Guillaumaud, N.;  
767 Bernard, L.; Clement, J.-C.; Poly, F. Variations in snow depth modify N-related soil  
768 microbial abundances and functioning during winter in subalpine grassland. *Soil Biol.*  
769 *Biochem.* **2016**, 92, 27–37.
- 770 (70) Hiltbrunner, E.; Schwikowski, M.; Körner, C. Inorganic nitrogen storage in alpine  
771 snow pack in the Central Alps (Switzerland). *Atmos. Environ.* **2005**, 39 (12), 2249–2259.
- 772 (71) Schmidt, S. K.; Lipson, D. A. Microbial growth under the snow: implications for  
773 nutrient and allelochemical availability in temperate soils. *Plant Soil* **2004**, 259 (1), 1–7.
- 774 (72) Williams, M. W.; Brooks, P. D.; Mosier, A.; Tonnessen, K. A. Mineral nitrogen  
775 transformations in and under seasonal snow in a high-elevation catchment in the Rocky  
776 Mountains, United States. *Water Resour. Res.* **1996**, 32 (10), 3161–3171.
- 777 (73) Saccone, P.; Morin, S.; Baptist, F.; Bonneville, J.-M.; Colace, M.-P.; Domine, F.;  
778 Faure, M.; Geremia, R.; Locht, J.; Poly, F.; et al. The effects of snowpack properties and  
779 plant strategies on litter decomposition during winter in subalpine meadows. *Plant Soil*  
780 **2013**, 363 (1–2), 215–229.
- 781 (74) Liu, F.; Williams, M. W.; Caine, N. Source waters and flow paths in an alpine  
782 catchment, Colorado Front Range, United States: SOURCE WATERS AND FLOW PATHS  
783 IN ALPINE CATCHMENTS. *Water Resour. Res.* **2004**, 40 (9).
- 784 (75) Cowie, R. M.; Knowles, J. F.; Dailey, K. R.; Williams, M. W.; Mills, T. J.; Molotch, N. P.  
785 Sources of streamflow along a headwater catchment elevational gradient. *J. Hydrol.*  
786 **2017**, 549, 163–178.
- 787 (76) Bodin, X.; Thibert, E.; Fabre, D.; Ribolini, A.; Schoeneich, P.; Francou, B.; Reynaud,

788 L.; Fort, M. Two decades of responses (1986–2006) to climate by the Laurichard rock  
789 glacier, French Alps. *Permafrost. Periglacial Process.* **2009**, *20* (4), 331–344.

790 (77) Williams, M. W.; Knauf, M.; Cory, R.; Caine, N.; Liu, F. Nitrate content and potential  
791 microbial signature of rock glacier outflow, Colorado Front Range. *Earth Surf. Process.*  
792 *Landf.* **2007**, *32* (7), 1032–1047.

793 (78) Saros, J. E.; Rose, K. C.; Clow, D. W.; Stephens, V. C.; Nurse, A. B.; Arnett, H. A.;  
794 Stone, J. R.; Williamson, C. E.; Wolfe, A. P. Melting Alpine Glaciers Enrich High-Elevation  
795 Lakes with Reactive Nitrogen. *Environ. Sci. Technol.* **2010**, *44* (13), 4891–4896.

796 (79) Slemmons, K. E. H.; Saros, J. E.; Simon, K. The influence of glacial meltwater on  
797 alpine aquatic ecosystems: a review. *Environ. Sci. Process. Impacts* **2013**, *15* (10), 1794.

798 (80) Williams, J. J.; Nurse, A.; Saros, J. E.; Riedel, J.; Beutel, M. Effects of glaciers on  
799 nutrient concentrations and phytoplankton in lakes within the Northern Cascades  
800 Mountains (USA). *Biogeochemistry* **2016**, *131* (3), 373–385.

801 (81) Hood, E.; Scott, D. Riverine organic matter and nutrients in southeast Alaska  
802 affected by glacial coverage. *Nat. Geosci.* **2008**, *1* (9), 583–587.

803 (82) Barnes, R. T.; Williams, M. W.; Parman, J. N.; Hill, K.; Caine, N. Thawing glacial and  
804 permafrost features contribute to nitrogen export from Green Lakes Valley, Colorado  
805 Front Range, USA. *Biogeochemistry* **2014**, *117* (2–3), 413–430.

806 (83) Louiseize, N. L.; Lafrenière, M. J.; Hastings, M. G. Stable isotopic evidence of  
807 enhanced export of microbially derived  $\text{NO}_3^-$  following active  
808 layer slope disturbance in the Canadian High Arctic. *Biogeochemistry* **2014**, *121* (3),  
809 565–580.

810 (84) Balestrini, R.; Arese, C.; Freppaz, M.; Buffagni, A. Catchment features controlling  
811 nitrogen dynamics in running waters above the tree line (central Italian Alps). *Hydrol.*  
812 *Earth Syst. Sci.* **2013**, *117* (3), 989–1001.

813 (85) Hall Jr, R. O.; Baker, M. A.; Arp, C. D.; Koch, B. J. Hydrologic control of  
814 nitrogen removal, storage and export in a mountain stream. *Limnol. Oceanogr.* **2009**, *54*,  
815 2128.

816 (86) Lovett, G. M.; Goodale, C. L. A New Conceptual Model of Nitrogen Saturation Based  
817 on Experimental Nitrogen Addition to an Oak Forest. *Ecosystems* **2011**, *14* (4), 615–631.

818 (87) Boutin, M.; Lamaze, T.; Couvidat, F.; Pornon, A. Subalpine Pyrenees received  
819 higher nitrogen deposition than predicted by EMEP and CHIMERE chemistry-transport  
820 models. *Sci. Rep.* **2015**, *5* (1).

821 (88) Hundey, E. J.; Russell, S. D.; Longstaffe, F. J.; Moser, K. A. Agriculture causes nitrate  
822 fertilization of remote alpine lakes. *Nat. Commun.* **2016**, *7*, 10571.

823 (89) Tsunogai, U.; Daita, S.; Komatsu, D. D.; Nakagawa, F.; Tanaka, A. Quantifying  
824 nitrate dynamics in an oligotrophic lake using  $\delta^{17}\text{O}$ . *Biogeosciences*  
825 **2011**, *8* (3), 687–702.

826 (90) Hobbs, W. O.; Lafrancois, B. M.; Stottlemyer, R.; Toczydlowski, D.; Engstrom, D. R.;  
827 Edlund, M. B.; Almendinger, J. E.; Strock, K. E.; VanderMeulen, D.; Elias, J. E.; et al.  
828 Nitrogen deposition to lakes in national parks of the western Great Lakes region:  
829 Isotopic signatures, watershed retention, and algal shifts: NITROGEN DEPOSITION TO  
830 NORTHERN LAKES. *Glob. Biogeochem. Cycles* **2016**, *30* (3), 514–533.

831 (91) Spaulding, S. A.; Otu, M. K.; Wolfe, A. P.; Baron, J. S. Paleolimnological Records of  
832 Nitrogen Deposition in Shallow, High-Elevation Lakes of Grand Teton National Park,  
833 Wyoming, U.S.A. *Arct. Antarct. Alp. Res.* **2015**, *47* (4), 703–717.

834 (92) Elser, J. J.; Andersen, T.; Baron, J. S.; Bergström, A.-K.; Jansson, M.; Kyle, M.; Nydick,  
835 K. R.; Steger, L.; Hessen, D. O. Shifts in lake N:P stoichiometry and nutrient limitation  
836 driven by atmospheric nitrogen deposition. *Science* **2009**, *326* (5954), 835–837.

837 (93) Bilbrough, C. J.; Welker, J. M.; Bowman, W. D. Early Spring Nitrogen Uptake by  
838 Snow-Covered Plants: A Comparison of Arctic and Alpine Plant Function under the  
839 Snowpack. *Arct. Antarct. Alp. Res.* **2000**, *32* (4), 404.

840 **List of Figures**

841

842 **Table 1** Mean volume-weighted concentration and concentration-weighted isotopic  
843 values for  $\text{NO}_3^-$  in snow pits (SP) and aerosols at the Lautaret Pass. Snow pits mean  
844 values are always calculated over the entire depth of the snow pack. Dates for SP  
845 are given in a dd/mm/yy format. SD is the standard deviation.

846

847 **Figure 1** Seasonal variations of a)  $\log([\text{NO}_3^-] \text{ in } \mu\text{g.L}^{-1})$  (for an easier comparison of  
848 streams  $[\text{NO}_3^-]$ ); b)  $\Delta^{17}\text{O}$  (‰) and corresponding  $f_{atm}$  (%), the relative amount of  
849 atmospheric nitrate in streams); c)  $\delta^{18}\text{O}$  (‰) and d)  $\delta^{15}\text{N}$  (‰) of  $\text{NO}_3^-$  in streams  
850 Red, blue and green colors stand for Tufiere, Laurichard and Romanche,  
851 respectively. Highlighted in yellow is a two-days rainstorm that occurred mid-June.  
852 The grey frames highlight the dormant season while the green one highlights the  
853 growing season. Transitions between both seasons are snowmelt period in spring,  
854 and plant senescence in autumn.

855



856 **Figure 2** Correlation between nitrate  $\Delta^{17}\text{O}$  (‰) and a), b), c)  $\log([\text{NO}_3^-])$ ; d), e), f)  
857  $\delta^{18}\text{O}$  (‰); g), h), i)  $\delta^{15}\text{N}$  (‰).

858 Red, blue and green colors stand for Tufiere, Laurichard and Romanche,  
859 respectively. Outliers (surrounded by stars) were not considered in the linear  
860 regression model, as we assume they result from biological processes (e.g.,  
861 denitrification) and would blur determination of  $\text{NO}_3^-$  sources.

862

863 **Figure 3** Dual isotopes plot ( $\Delta^{17}\text{O}$  vs.  $\delta^{15}\text{N}$ ) illustrating the mixing between three  
864 sources of  $\text{NO}_3^-$  in our study sites. The plain triangles feature the mixing range  
865 between snow  $\text{NO}_3^-_{atm}$  and  $\text{NO}_3^-$  from nitrified  $\text{NH}_4^+_{atm}$  in grey,  $\text{NO}_3^-$  from nitrified  
866  $\text{NH}_4^+_{bio}$  in turquoise and  $\text{NO}_3^-$  from manure or sewage in beige. The dashed triangles  
867 of similar colors (i.e., grey-turquoise and turquoise-beige) illustrate the overlapping of  
868 sources  $\delta^{15}\text{N}$ - $\text{NO}_3^-$  values. The dashed purple triangle illustrates the mixing range  
869 between  $\text{NO}_3^-_{atm}$  and  $\text{NO}_3^-$  from nitrified  $\text{NH}_4^+_{bio}$  if summer deposition was the  
870 atmospheric end-member.

871 When  $\Delta^{17}\text{O}$ - $\text{NO}_3^-$  values are high,  $\delta^{15}\text{N}$ - $\text{NO}_3^-$  is characteristic of nitrified  $\text{NH}_4^+_{atm}$ ,  
872 delineating the coupled contribution of atmospheric N deposition *via* direct inputs  
873 ( $\text{NO}_3^-_{atm}$ ) and indirect inputs (nitrified  $\text{NH}_4^+_{atm}$ ). Decreased contribution of atmospheric  
874 N sources (low  $\Delta^{17}\text{O}$ - $\text{NO}_3^-$  values) results in a higher proportion of  $\text{NO}_3^-_{bio}$ .

|                      | Snow<br>depth (cm) | $\delta^{15}\text{N}$ (‰) | $\delta^{18}\text{O}$ (‰) | $\Delta^{17}\text{O}$ (‰) | $[\text{NO}_3^-]$ (mg.L <sup>-1</sup> ) |
|----------------------|--------------------|---------------------------|---------------------------|---------------------------|---|
|                      |                    | Mean (SD)                 | Mean (SD)                 | Mean (SD)                 | Mean (SD)                               |
| SP 09/12/14          | 66                 | -5.5 (2.7)                | 77.0 (5.0)                | 29.8 (1.9)                | 0.1 (0.4)                               |
| SP 13/01/15          | 64                 | -3.6 (1.7)                | 76.6 (7.2)                | 28.6 (2.5)                | 0.1 (0.9)                               |
| SP 19/02/15          | 139                | -2.4 (1.2)                | 77.7 (4.5)                | 29.3 (1.2)                | 1.2 (1.3)                               |
| SP 19/03/15          | 142                | -2.3 (1.6)                | 76.3 (4.6)                | 28.5 (1.3)                | 0.9 (1.0)                               |
| SP 09/04/15          | 104                | -4.1 (1.1)                | 77.2 (6.8)                | 30.1 (1.0)                | 0.6 (0.6)                               |
| Aerosols<br>(summer) | -                  | -6.5 (3.6)                | 62.9 (6.5)                | 23.1 (2.4)                | 0.1 (0.1) mg.m <sup>-3</sup>            |
| Aerosols<br>(winter) | -                  | -1.0 (1.7)                | 74.7 (4.4)                | 28.9 (1.0)                | 0.1 (0.2) mg.m <sup>-3</sup>            |

**Table 1**

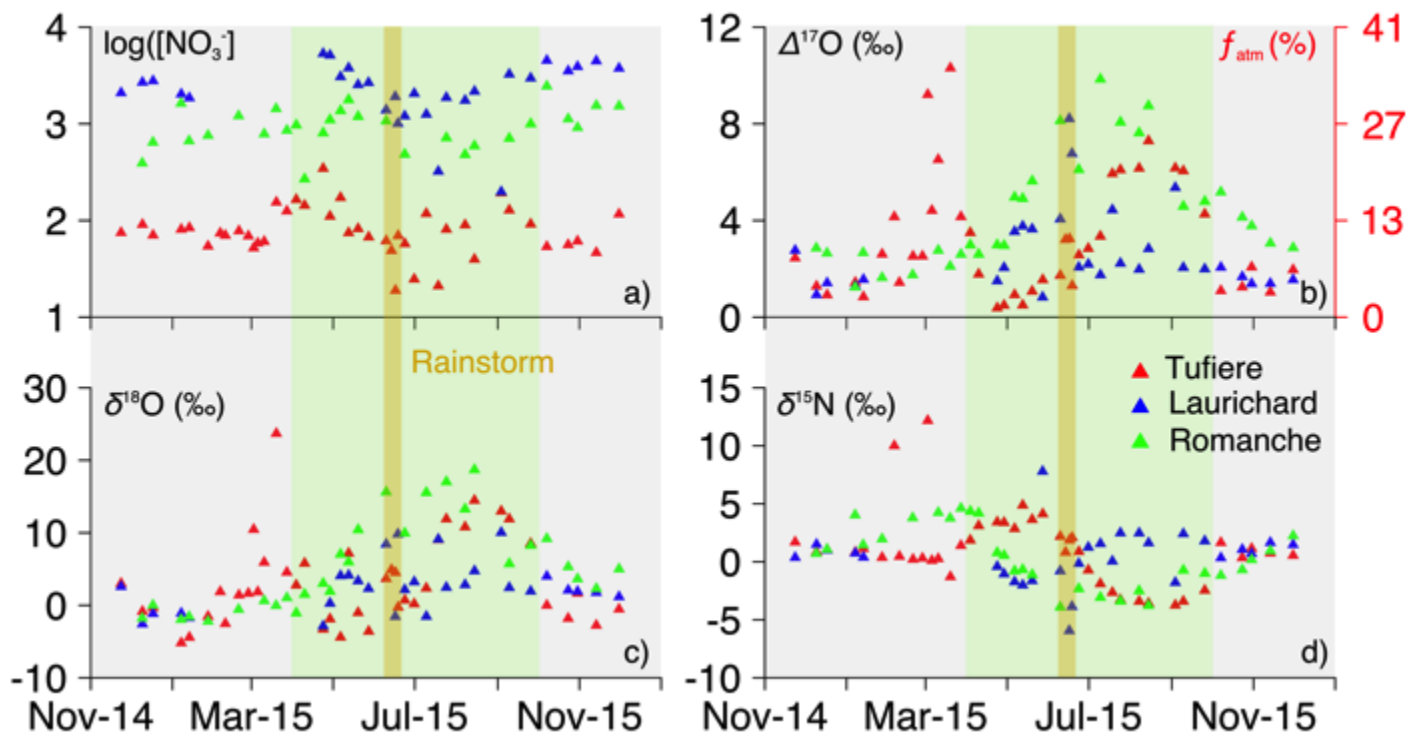


Figure 1

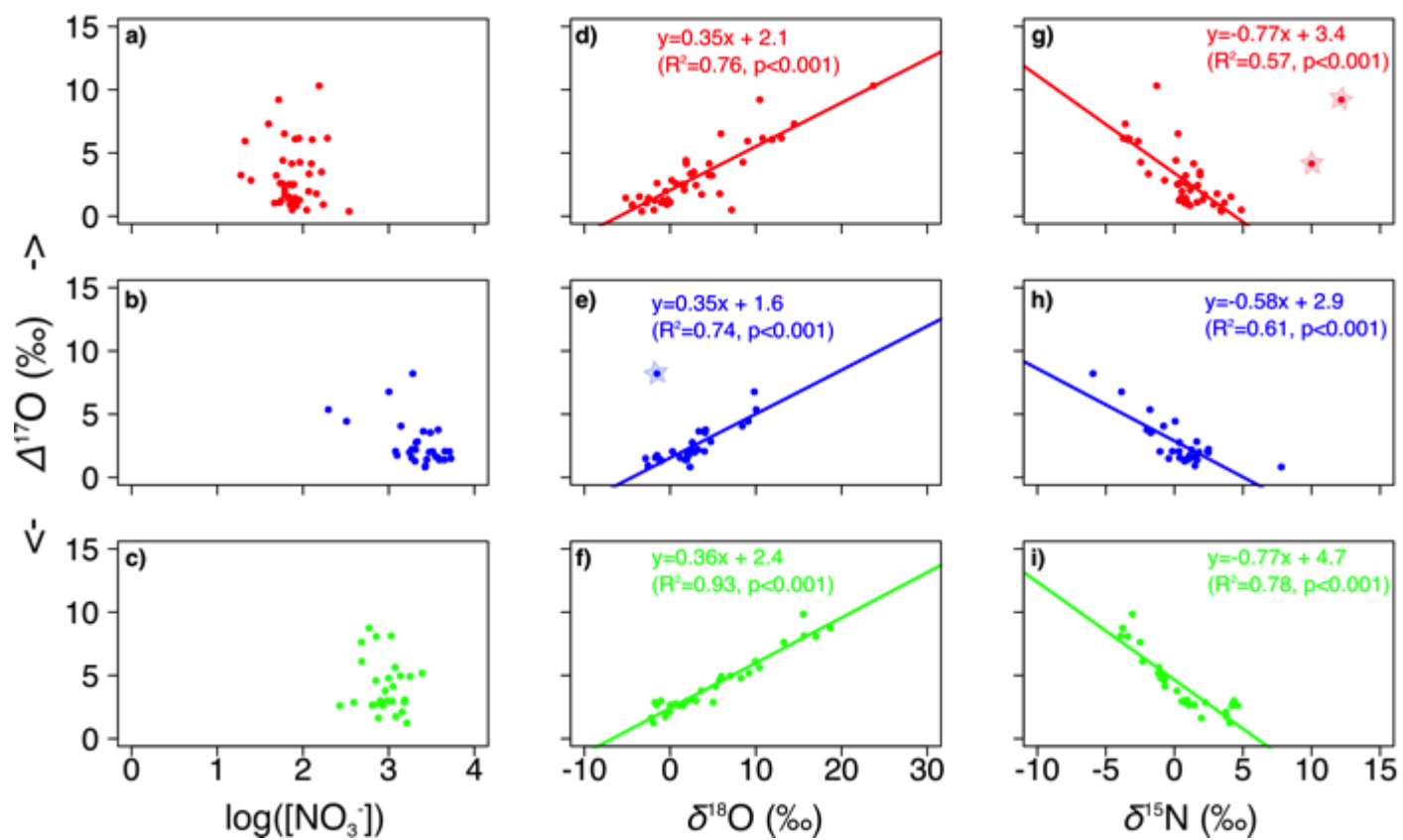


Figure 2

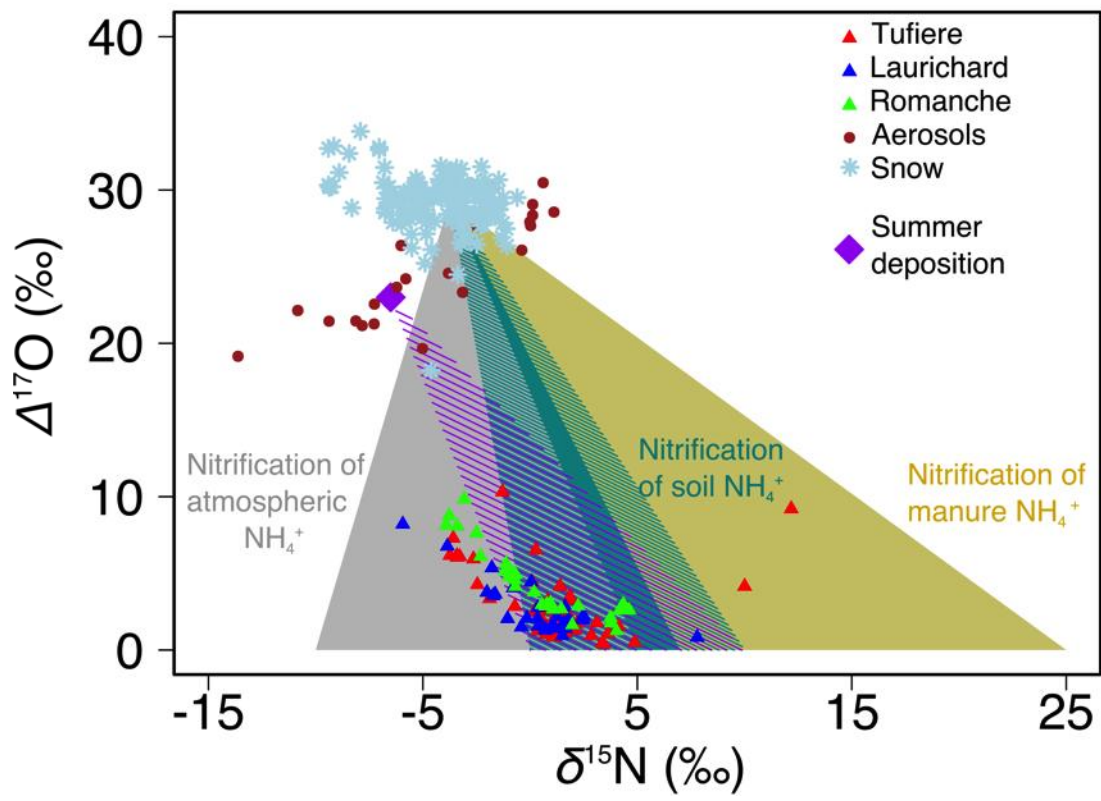


Figure 3